Research Article | Vol. 27, No. 7 | 1 Apr 2019 | OPTICS EXPRESS 9631
Optics EXPRESS

Flexible fabrication of micro-optics arrays with high-aspect-ratio by an offset-tool-servo diamond machining system

ZHANWEN SUN,[1] SUET TO,[1,*] GUOQING ZHANG,[2] AND SHAOJIAN ZHANG[3]

[1]*State Key Laboratory in Ultra-Precision Machining Technology, Department of Industrial and Systems Engineering, The Hong Kong Polytechnic University, Kowloon, Hong Kong*
[2]*Guangdong Provincial Key Laboratory of Micro/Nano Optomechatronics Engineering, College of Mechatronics and Control Engineering, Shenzhen University, Shenzhen, Guangdong, China*
[3]*Research Institute of Mechanical Manufacturing Engineering, School of Mechatronics Engineering, Nanchang University, Nanchang, Jiangxi, China*
**sandy.to@ polyu.edu.hk*

Abstract: Micro-optics arrays (MOAs) with high aspect ratio (AR) have unique advantages in realizing the minimization of optical systems by reducing the focal distance. Fast or slow tool servo (F/STS) is widely regarded as an outperforming technique for the fabrication of MOAs featuring high form accuracy. However, in the machining of MOAs with high AR, the non-smooth cutting trajectory of F/STS inevitably leads to intensive tool vibrations and the interference between the tool flank face and the finished surface, thereby deteriorating surface roughness. In this study, a novel offset-tool-servo (OTS) diamond machining technology and the corresponding toolpath generation algorithm are proposed to achieve the flexible fabrication of micro-freeform lens arrays with high AR. In OTS, with the assistance of four-axis servo motions, a spiral toolpath is generated for each single lenslet, which effectively avoids the tool interference induced by the steep descending movement of the tool in F/STS. Besides, the proposed machining strategy well ensures the smoothness of the generated toolpath for each lenslet, thereby effectively avoiding the destruction of the surface quality induced by the tool vibrations. In practice, this method is validated by fabricating different MOAs with aspheric and freeform structures. Compared with F/STS, the OTS method is demonstrated to be able to achieve two times larger AR values, and smoother and more uniform surface quality are simultaneously achieved.

© 2019 Optical Society of America under the terms of the OSA Open Access Publishing Agreement

1. Introduction

Micro-optics arrays (MOAs) containing a large number of lenslet cells have been widely applied in cameras, sensors and photonic devices, due to its superior performance in large visual field and minimization in size [1,2]. Originally, the lenslet has been designed into spheric and aspheric surfaces [3]. Recently, with the fast development of optical and electronical devices, these simple surfaces are hard to fulfill the requirements of advanced optical systems for multi-function integration [4,5]. Instead, MOAs featuring complicated structures has received more and more attentions, such as micro-Fresnel lens arrays [5], compound eye structures [6], micro-grating arrays [7] and retroreflective arrays [4]. These MOAs generally feature high aspect ratio (AR) and discontinuous structures with ultra-high form accuracy. MOAs with high AR as well as complicated structures provide inconceivable imaginations to optical designers to realize multi-function integration and minimization of optics systems. However, the complex shapes with high AR of the lenslet impose great challenges for current machining technologies on cost-effective fabrication of these MOAs with ultra-smooth surface roughness and ultra-high form accuracy.

To fulfill the requirements of MOAs, different micro manufacturing techniques have been proposed, which can be roughly divided into non-mechanical and mechanical machining. The

#355332 https://doi.org/10.1364/OE.27.009631
Journal © 2019 Received 13 Dec 2018; revised 3 Feb 2019; accepted 11 Feb 2019; published 20 Mar 2019

non-mechanical machining, dominated by chemical etching [8] and laser lithography [9], can achieve large-scale fabrication of MOAs. Nevertheless, these techniques commonly require expensive facilities and complex operations with high cost, as well as are restricted to process specific materials with limited geometric complexity [10,11]. Mechanical machining using diamond tools are widely regarded as more promising for flexible fabrication of MOAs with complicated structures on a wide range of engineering materials, due to its superiority in achieving ultra-high form accuracy.

According to the tool configuration strategy, mechanical machining can be classified into fast and slow tool servo (F/STS) diamond turning and diamond milling [12–14]. In diamond milling, a ball milling tool is mounted on a high-speed spindle. Rotationally symmetric lenslet can be individually generated by the rotational diamond tool. With the assistance of three translational servo motions, the whole workpiece surface can be covered by machining lenslet cells one by one. In this way, uniform surface quality can be achieved on the whole MOAs surface due to the consistent cutting conditions for each lenslet. However, diamond milling is restricted to producing large sparse arrays with simple spheric or aspheric shape [15]. It is hard to satisfy the increasing demands for the MOAs with high AR as well as with arbitrary shapes.

F/STS diamond turning has been demonstrated to be the outperforming method for fabrication of MOAs with ultra-high form accuracy [13,16]. With the assistance of the high frequent servo motion along *Z*-axis, lenslet featuring aspheric or even freeform shapes can be flexibly fabricated on a wide range of engineering materials. Nevertheless, in F/STS diamond turning of MOAs, the inevitable discontinuous toolpath can induce severe tool vibrations, thereby deteriorating surface roughness and resulting in poor surface quality [16,17]. Especially, the tool vibrations can be more obvious in the machining of MOAs with high AR, owing to the steep descending and rising movements of the diamond tool [18]. Moreover, the non-smooth toolpath with large slope angle in turning of MOAs with high AR inevitably cause the interference between the flank face of the diamond tool and the finished surface [19]. Even though F/STS is a promising technique for the generation of micro-structures, all the aforementioned issues restrict its application in the fabrication for MOAs with high AR as well as with complicated structures.

Developed from F/STS, several diamond machining technologies have been proposed for the generation of MOAs with specific shapes. For example, polygonal Fresnel lens arrays have been fabricated by Neo DWK et al. [20] using an innovative diamond micro chiseling method. Guilloche machining technology has been proposed by Brinksmeier et al. [4] to fabricated retroreflective arrays. Nevertheless, these methods are only applicable to fabricate MOAs with the aforementioned shapes, thereby having very limited flexibility. To achieve large-scale fabrication of MOAs, a technique named end-fly-cutting-servo has been proposed by Zhu et al. [21]. This method well ensures the uniformity of the surface quality in a large area, and can also be applied to fabricated hybrid MOAs [17]. Nevertheless, the toolpath of the end-fly-cutting-servo system is also non-smooth in the generation of MOAs just like conventional F/STS, so this method is also restricted to fabricating MOAs with high AR due to the tool interference and vibration.

To achieve the flexible fabrication of discontinuously structured micro-optics arrays, a virtual spindle based tool servo diamond turning technology has been proposed by Zhu et al. [18]. In virtual spindle turning, the workpiece is attached on the spindle following the rotational motion of the *C*-axis, while the diamond tool is fixed on a tool holder and then clamped on the *Z* translational slide. Arrayed micro-structures with uniform surface quality can be generated by this method through virtually constructing the rotation axis at the centers of all lenslet cells in sequence. However, to make the center of each lenslet cell be always coincident with the constructed virtual spindle, harmonic oscillations with the same frequency of that of the spindle rotation are necessarily assigned to *X*- and *Y*-axis. As the workpiece is fixed on the spindle in virtual spindle turning, very high oscillation amplitudes are required

for *X*- and *Y*-axis in the machining of MOAs with large aperture, which strongly challenges the dynamic response of the machining tools. In addition, very slow spindle rotation rate should be adopted to reduce the oscillation frequency, which accordingly is low-efficient.

In various optical applications, the aspect ratio of MOAs generally ranges from 0.02 to even 0.23 [16,17,22]. Currently, due to the various machining technologies, there is no consistent criteria that clearly defines the high and low AR for MOAs. For example, for the MOAs generated by mechanical machining methods, such as F/STS, sculpturing and milling, the aspect ratio is generally less than 0.06 to avoid the interference between the tool and the lenslet cell [19]. In order to generate MOAs with the AR higher than 0.06, non-mechanical machining technologies, such as LIGA and laser machining, are required [22,23]. However, these non-mechanical techniques commonly require complex operations with low efficiency, as well as are restricted to processing specific materials with limited geometric complexity and with limited form accuracy. Based on the state-of-art of current machining techniques, the AR of 0.06 can be regarded as a boundary between high and low AR for mechanical machining technologies.

To overcome the difficulties for current diamond cutting technologies in the fabrication of MOAs with high AR, a novel offset-tool-servo (OTS) diamond machining technique is proposed in the present study. The basic idea of OTS is the combination of the concepts of ball milling and F/STS. With the assistance of the four-axis servo motions, spiral toolpath is generated for each lenslet cell, which effectively avoid the tool interference and vibration in the machining of MOAs with high AR. This machining approach also offers good flexibility for the generation of MOAs featuring complicated structures. Toolpath determination strategy is introduced with the consideration of the unique machining principle of OTS. To validate the proposed OTS, two types of MOAs, namely MOAs with aspheric and with micro-freeform surfaces, are generated, and the experimental results are compared with that of conventional F/STS.

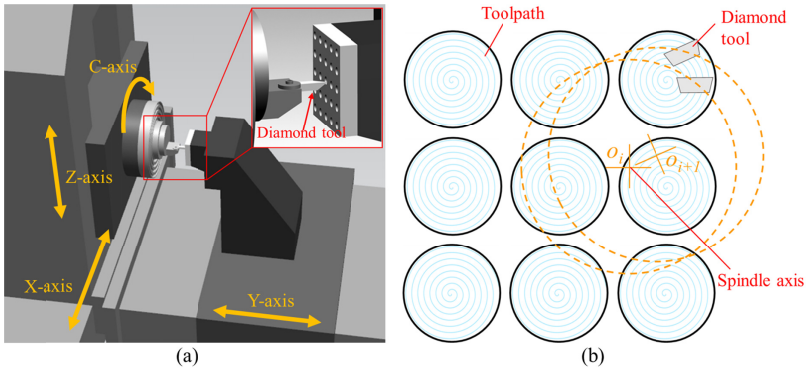

Fig. 1. Schematics of (a) the configuration of the OTS and (b) the basic machining principle.

2. Principle for flexible generation of MOAs

To avoid the interference between the tool flank surface and the finished surfaces in diamond turning, the clearance angle of the diamond tool is required to be larger than the maximum slope angle of the desired surface along the toolpath. Accordingly, the diamond tool with a large clearance angle is generally adopted in F/STS turning of MOAs with high AR to avoid the tool interference [24]. Nevertheless, the large clearance angle highly reduces the stiffness of the tool tip, thereby resulting in extensive tool vibrations especially under the frequent acceleration and deceleration movements in F/STS. Without reducing the tool stiffness, an alternative solution is adopted in the proposed offset-tool-servo (OTS) system through separately machining each lenslet using an independent spiral toolpath. The basic principle of

OTS system is to synthesize the advantages of ball end milling and F/STS by using multi-axis servo motions including *X*-, *Y*-, *Z*- and *C*-axis.

The schematic configuration of the OTS system is shown in Fig. 1(a). Different form conventional F/STS, the diamond tool is fixed on the spindle via a tool holder. The workpiece is clamped on the fixture that is installed on the *Z*-slide to realize the translational servo motion along *Z*-axis. Through the rotary movement of spindle, the direction of the tool rake face can be flexibly adjusted to be perpendicular to the projected toolpath. As there exists a fixed offset distance between the tool tip and the spindle axis, the rotational spindle generates a circular trajectory of the diamond tool as the yellow dashed-lines shown in Fig. 1(b). With the cooperative servo motions along *X*- and *Y*-axis directions, the circular trajectories can be shifted to a set of spiral toolpaths for each lenslet, just like ball end milling, as the blue lines shown in Fig. 1(b). The translational servo motion of the workpiece along *Z*-axis is used to deterministic generation of the desired shapes of each lenslet and compensation of tool edge radius, just like F/STS. By separately fabricating each lenslet cell at different locations on the workpiece, the whole MOAs can be acquired. Overall, in OTS, the combination of the servo motions in *X*-, *Y*- and *C*-axis determines the spiral toolpath as well as adjusts the cutting direction of the diamond tool, while the servo motion in *Z*-axis is responsible for the generation of the desired lenslet surface.

The unique machining strategy of OTS achieves the following advantages in the fabrication of MOAs:

(i) Avoidance of the tool interference in the machining MOAs with large AR. In OTS system, the lenslet is individually machined under the spiral toolpath. The center of each spiral toolpath overlaps to the center of the corresponding lenslet, as shown in Fig. 1(b). In this case, the slope angle of the toolpath is determined by the curvature change of the toolpath, instead of the aspect ratio of the lenslet. Figure 2(a) shows the relative position between the diamond tool and the generated lenslet in OTS system from the view of cross-sectional direction. It is seen that the slope angle of the toolpath at the cutting point is 0° and irrelevant to the AR of the lenslet. In comparison, the center of the spiral toolpath for F/STS technology is located at the center of the workpiece. Thus, very large slope angle can be generated at the points where the diamond tool is cutting into the lenslet from the primary surface, as shown in Fig. 2(b). This very large slop angle can cause the tool interference on the flank face, especially in the machining of MOA with high AR.

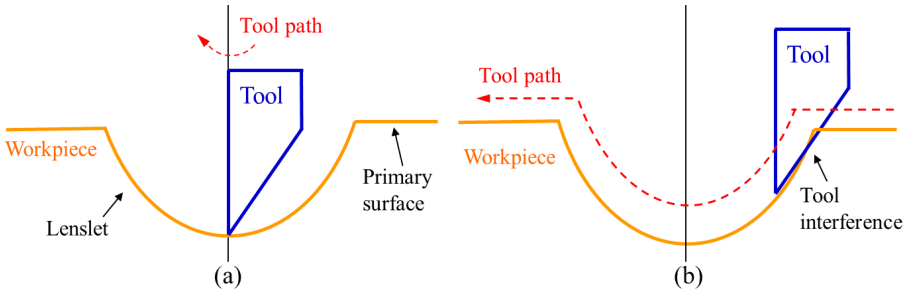

Fig. 2. Relative position between the diamond tool and the lenslet generated by (a) OTS system and (b) F/STS system.

With the consideration of the tool interference at the bottom of the lenslet, the maximum allowable AR for the lenslet generated by OTS can be calculated by $\tan(\alpha)$, where α is the clearance angle of the diamond tool. In contrast, the maximum allowable AR for the lenslet generated by F/STS need to be less than $1/\sin(\alpha)$-$1/\tan(\alpha)$ to avoid the interference of the tool flank face [19]. For example, using the diamond tool with a clearance angel of 7°, MOAs with the AR of $\tan(7°) = 0.122$ can be machined by OTS, which cannot be

fabricated by the conventional F/STS due to the tool interference. Using the same diamond tool, the maximum AR that can be achieved by F/STS is only 1/sin(7°)-1/tan(7°) = 0.061.

(ii) Avoidance of the tool vibration. In OTS system, the toolpath is smooth and continuous without frequent acceleration and deceleration movements, which effectively suppress the tool vibration. Besides, the cutting speed for each lenslet is constant, so uniform surface quality for the whole optic arrays can be acquired. In contrast, discontinuous toolpath with impulse excitations inevitably happen in F/STS system when the tool cuts into and out of the lenslet, which will lead to severe tool vibrations and destroy the surface quality, which will be experimentally validated below.

(iii) Flexibility in machining of MOAs with large apertures. in OTS, as the offset distance of the diamond tool with respect to the rotation center of the spindle is fixed, the oscillation amplitudes of *X*- and *Y*-axis are also fixed and have no relationship with the aperture of the workpiece. Accordingly, the proposed OTS method is flexible to fabricate optic components with very large aperture, without influencing the dynamic response of the machine tools. Through adopting a very small offset distance, high rotation speed rate can be selected to increase the machining efficiency.

Overall, the unique cutting process of the proposed OTS system make this machining strategy has the advantage in machining micro-optics arrays with high AR as well as in machining micro-freeform optics with complicated structures. The alleged advantages will be further demonstrated in the following part.

3. Toolpath determination for the OTS

In OTS, each micro lenslet cell is independently generated, so the whole lenslet arrays can be obtained by repeating the basic cutting operation for the single lenslet cell at the corresponding places of the lenslet arrays. In the machining process, the spiral toolpath for a single lenslet cell is decomposed into the servo motions of four axes, including three translational motions and a rotary motion. Besides, the rake face of the diamond tool should remain perpendicular to the projected toolpath. Through analyzing the kinematics of the OTS system, toolpath generation strategy is proposed.

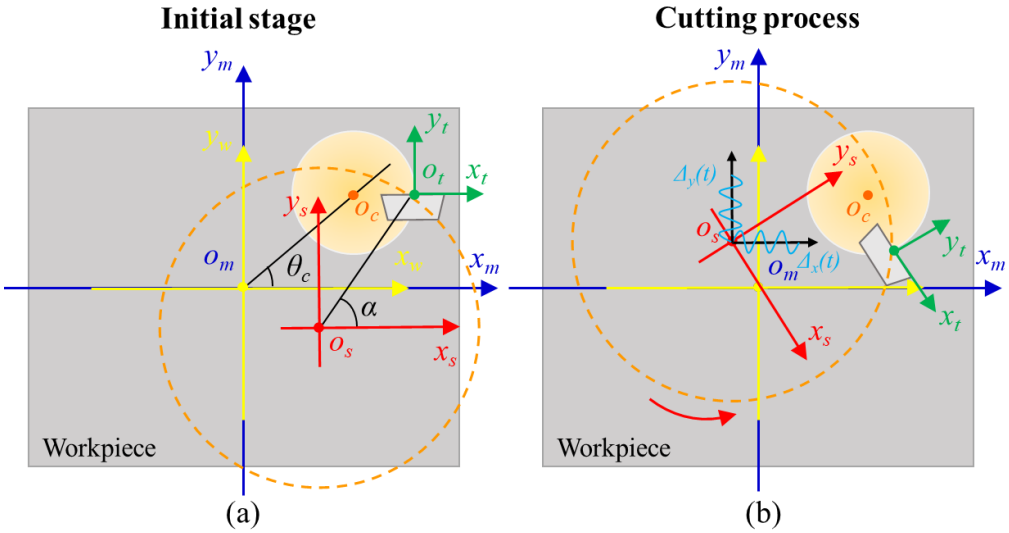

Fig. 3. Schematic of the kinematics of the OST machining for a single lenslet cell in (a) initial stage and (b) cutting process.

3.1 Kinematics of the OTS

Without loss of generality, the kinematics of the OTS in the machining of one lenslet cell is illustrated in Fig. 3. The coordinate systems o_m-$x_m y_m z_m$ and o_w-$x_w y_w z_w$ are assigned to the machine tool and the workpiece, respectively. The two coordinates overlap to each other at the initial stage, with the x_w- and x_m-axis are set in the horizontal direction, as shown in Fig. 3(a). During machining, o_m-$x_m y_m z_m$ is unchanged and serve as the spatial reference. o_t-$x_t y_t z_t$ is the coordinate system that is fixed on the cutter location point (*CLP*), with y_t-axis is set as perpendicular to the tool rake face. Before the machining process, the tool rake face is set to be horizontal with the assistance of the linear variable differential transformer. In practice, there is a is a fixed offset distance ρ and a fixed angle discrepancy α between the diamond tool and the rotation center of the spindle. o_s-$x_s y_s z_s$ is the coordinate system of the spindle, with original point o_s is set to the spindle center. Thus, o_t-$x_t y_t z_t$ and o_s-$x_s y_s z_s$ rotates with the rotational spindle and there are no relative motions between the two coordinates.

At the initial stage of machining as shown in Fig. 3(a), the *CLP* is moved to the right side of the lenslet cell through the translational motions of *X*- and *Y*-axis. In the cutting process, the spindle rotates with a constant speed, and the *X*- and *Y*-axis harmonically move back and forth in the same frequency to generate a local circular trajectory with its center fixed at the point o_c, as shown in Fig. 3(b). Then, through the feed movement of the *X*-axis, local spiral toolpath with constant feed rate per revolution can be generated for the lenslet cell. The servo movement along the *Z*-axis is responsible for the generation of the desired shape of the lenslet as well as for the tool edge compensation. By repeating the operations for the generation of the single lenslet cell at different locations on the workpiece, the whole MOAs can be acquired.

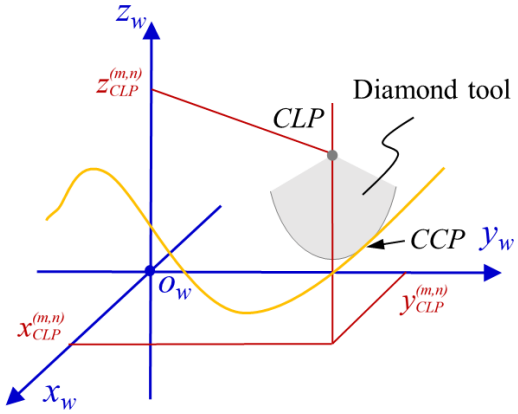

Fig. 4. Schematic of the determination of *CCP* in the o_w-$x_w y_w z_w$ system.

3.2 Toolpath determination

Assume that the desired lenslet cell has a radius of r_c and the coordinate of its center point o_c is (a,b) in the workpiece coordinate system, as shown in Fig. 3(a). Constant angle sampling strategy is adopted by uniformly discretizing the rotational angle of spindly into (N_s + 1) points for each revolution. For the n-th point of the m-th revolution, the rotation angle of the spindle can be expressed as:

$$\varphi_{m,n} = 2\pi m + \frac{2\pi n}{N_s} \tag{1}$$

During the machining, rake face of the diamond tool should remain perpendicular to the projected toolpath, so the line of x_t-axis remains passing through the center point of the lenslet

cell o_c. Based on this geometric relation, the coordinate of the *CLP* corresponding to $\varphi_{m,n}$ can be expressed in the system o_m-$x_m y_m z_m$ by:

$$\begin{cases} x_{CLP}^{(m,n)} = -d_c \cos(\theta_c + \varphi_{m,n}) - d_c + \dfrac{\varphi_{m,n} f_e}{2\pi} \\ y_{CLP}^{(m,n)} = -d_c \sin(\theta_c + \varphi_{m,n}) \end{cases} \tag{2}$$

where f_e is the feed rate, d_c and θ_c are the distance between the o_c to o_m and the angel between line $o_c o_m$ and x_m-axis, as shown in Fig. 3(a), which can be expressed by:

$$\begin{cases} d_c = \sqrt{(a^2 + b^2)} \\ \theta_c = \arctan(b / a) \end{cases} \tag{3}$$

Assuming that a diamond tool with rake angle of 0° and edge radius of R_t is adopted, the tool edge profile corresponding to rotation angle $\varphi_{m,n}$ can be expressed in the system o_m-$x_m y_m z_m$ by:

$$\begin{cases} x_T^{(m,n)} = -x_{CLP}^{(m,n)} + l \times \cos(\varphi_{m,n}) \\ y_T^{(m,n)} = -y_{CLP}^{(m,n)} + l \times \sin(\varphi_{m,n}), l = [-R_t \cos(\delta), R_t \cos(\delta)] \\ z_T^{(m,n)} = z_0 - \sqrt{R_t^2 - l^2} \end{cases} \tag{4}$$

Where δ is the wrap angle of the diamond tool. The cutting edge is then uniformly discretized into (N_0 + 1) points to conduct numerical calculation. The tangent vector of the i-th point (x (m,n) T,i, y (m,n) T,i, z (m,n) T,i) can be expressed as:

$$\begin{aligned} \vec{T}_i &= \left(\frac{\partial x_T^{(m,n)}}{\partial l}, \frac{\partial y_T^{(m,n)}}{\partial l}, \frac{\partial z_T^{(m,n)}}{\partial l}\right) \Big| \, l = l_i \\ l_i &= --R_t \cos(\delta) + (i-1)\frac{2R_t \cos(\delta)}{N_0} \end{aligned} \tag{5}$$

The surface of the lenslet cell can be expressed in the o_w-$x_w y_w z_w$ system is expressed $z_w = F_w(x_w, y_w)$. The normal vector of the surface corresponding to the i-th point of the cutting edge can be expressed by:

$$\vec{V}_i = \left(\frac{\partial F_w}{\partial x}, \frac{\partial F_w}{\partial y}, -1\right) \Big| \, x = x_{T,i}^{(m,n)}, y = y_{T,i}^{(m,n)} \tag{6}$$

The cutter contact point (*CCP*) can be determined by finding a position where the tool edge is tangential to the lenslet surface, as shown in Fig. 4. Thus, *CCP* can be approximately determined by the numerical calculation of the minimum value of the tow vectors [25]:

$$d_T^{(m,n)} = \arg\min_{l_i} \left\{ \left| \vec{V}_i \times \vec{T}_i \right|, \forall i \in [1, N_0 + 1] \right\} \tag{7}$$

The coordinate of *CLP* at the rotation angle $\varphi_{m,n}$ in the o_m-$x_m y_m z_m$ system can be expressed by:

$$\begin{cases} x_{CLP}^{(m,n)} = -d_c \cos(\theta_c + \varphi_{m,n}) - d_c + \varphi_{m,n} f_e / 2\pi \\ y_{CLP}^{(m,n)} = -d_c \sin(\theta_c + \varphi_{m,n}) \\ z_{CLP}^{(m,n)} = \sqrt{R_t^2 - l_i^2} + F_w\left[-x_{CLP}^{(m,n)} + l_i \times \cos(\varphi_{m,n}), -y_{CLP}^{(m,n)} + l_i \times \sin(\varphi_{m,n})\right] \end{cases} \tag{8}$$

As the diamond tool is fixed on the spindle with a fixed offset distance with respect to the rotation center, so there is no relative motion between the ordinances o_t-$x_t y_t z_t$ and o_s-$x_s y_s z_s$. As

a result, *CLP* can be projected by deliberately controlling the coordinate of center point of the spindle o_s. Through matrix for coordinate transform, the coordinate of the point o_s in the o_m-$x_m y_m z_m$ can be expressed by:

$$\begin{pmatrix} x_s^{(m,n)} \\ y_s^{(m,n)} \\ z_s^{(m,n)} \\ 1 \end{pmatrix} = \begin{pmatrix} 1 & 0 & 0 & -\rho\cos(\alpha) \\ 0 & 1 & 0 & -\rho\sin(\alpha) \\ 0 & 0 & 1 & 0 \\ 0 & 0 & 0 & 1 \end{pmatrix} \times \begin{pmatrix} x_{CLP}^{(m,n)} \\ y_{CLP}^{(m,n)} \\ z_{CLP}^{(m,n)} \\ 1 \end{pmatrix} \tag{9}$$

The toolpath can be determined by repeating the aforementioned calculations through out all *m* and *n*. In machining process, the spindle rotates with a constant speed. *X*-, *Y*- and *Z*-axis moves in the servo mode according to the points *x* (*m,n*) *s, y* (*m,n*) *s* and *z* (*m,n*) *s*, respectively. Then, by repeating this operation in the at the corresponding places of the lenslet arrays, MOAs with desired shapes can be acquired.

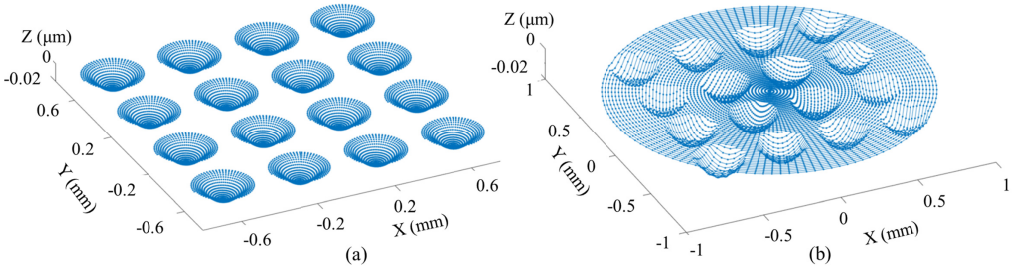

Fig. 5. Characteristics of the toolpath for (a) OTS and (b) F/STS.

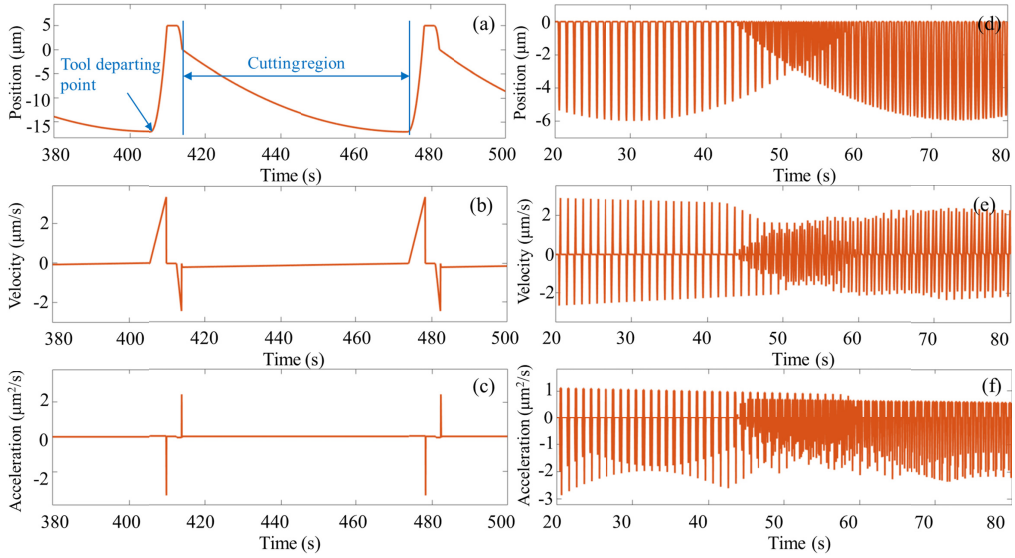

Fig. 6. Dynamic characteristics of the tool motions in *Z*-axis for OTS: (a) position, (b) velocity and (c) acceleration and for F/STS (d) position, (e) velocity and (f) acceleration.

3.3 Characteristics of the toolpath

To provide an intuitionistic description of the machining characteristics of OTS system, the toolpath for a typical MOAs is generated, as shown in Fig. 5(a). The circumradius and the depth of each lenslet cell is 150 μm of 17 μm, respectively. It is seen that the toolpath for OTS is characterized as a set of independent spiral trajectories with constant interval per

revolution. The center of each spiral trajectory is consistent with the center of the corresponding lenslet of the MOAs. The independent cutting process of OTS effectively avoids tool vibration and enhance the uniformity of the surface quality for each lenslet. In contrast, the toolpath for F/STS is characterized as a single spiral trajectory with its center located at the center of the MOAs, as shown in Fig. 5(b). In this case, more than one lenslet cell is covered during one rotation of the spindle. Steep descending movement of the diamond tool is required at the points where the diamond tool cuts into each lenslet from the primary surface, which can lead to tool interference of the flank face and severe tool vibrations. The tool vibrations can be more intensive at the position with larger radial distance, as more lenslet cell is covered per revolution here.

A comparison of the dynamic characteristics of the tool motion along *Z*-axis between the proposed OTS and F/STS are shown in Fig. 6, including position, velocity and acceleration. As shown in Fig. 6(a), in OTS, the diamond tool periodically contacts and departs from the workpiece, but the toolpath in the cutting region is very smooth. As shown in Fig. 6(b) and 6(c), there is no velocity and acceleration fluctuations during the cutting process. In contrast, in F/STS, the tool remains contact with the workpiece, and intensive fluctuations of the velocity and acceleration can be observed during cutting process, as shown in Figs. 6(e) and 6(f). This is because that in F/STS, each lenslet can be treated as an impulse excitation for the diamond tool. The intensive tool vibrations induced by the discontinuous impulses can destroy the surface quality. Overall, compared with the conventional F/STS, the OTS strategy can be used to generate MOAs with higher AR without tool interference as well as can effectively suppress the tool vibrations.

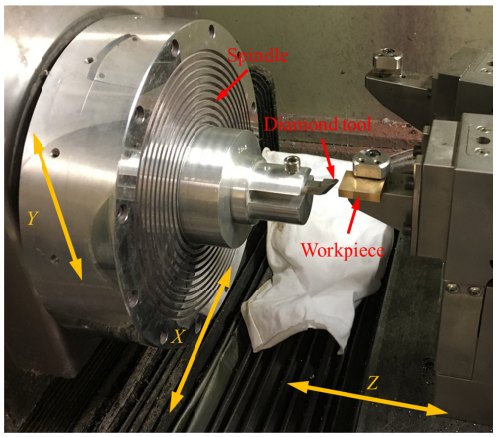

Fig. 7. Hardware configuration of the OTS system.

Table 1. Coeffecients of the micro-aspheric surface generated by OTA and STS.

Coefficient	OTS	STS
Shape coefficient *s*	–1	–1
Radius of the array R_0 (mm)	0.15	0.15
Conic constant *k*	–0.6	–0.6
Curvature *C* (mm^{-1})	5.7	2.5
Aspect ratio	0.11	0.04

4. Experimental setup

A four-axis ultra-precision turning machine (Moore 350FG, USA) is used in the experiments, as shown in Fig. 7. The turning machine is equipped by a spindle and three translational slides. The workpiece is clamped on the *Z* slide, while diamond tool is fixed on a tool holder

and then absorbed on the spindle via the vacuum chuck. In the machining, the spindle and the three translational slides works under servo motion mode. The workpiece material is copper. A diamond tool provided by Contour company is adopted. The tool nose radius is 0.28 mm and the rake and clearance angle are 0° and 7°, respectively. To observe the shape and micro-topogriphies of the machined surface, a non-contact optical measurement system (Zygo Nexview) is used under proper magnification. An optical micro-scope (Olympus BX60) is also used to capture the topographies of the machined structures.

Table 2. Machining parameters for OTS and STS.

Machining parameters	Hybrid micro-aspheric surface	Hybrid sinusoid surface
Spindle rotation rate (rpm)	15	30
Feed rate (μm/r)	2	2
Depth of cut (μm)	5	5
Offset radius (mm)	5.45	none

To validate the advantages of the proposed OTS in machining of MOAs with high AR, micro-aspheric arrays were fabricated using OTS, and the results were compared with that generated by F/STS. The expression of the micro-aspheric lenslet is [26]:

$$z(x,y)=\frac{sCR_0^{\ 2}}{4+4\sqrt{1-(1+k)C^2R_0^{\ 2}}}-\frac{sC\rho^2(x,y)}{4+4\sqrt{1-(1+k)C^2\rho^2(x,y)}} \tag{10}$$

where R_0 denotes the aspheric radius; k and C controls the conicity and the curvature, respectively; s is the shape coefficient. As discussed above, the highest AR that can be achieved by OTS is 0.122 using a tool with 7° clearance angle, while only 0.061 can be achieved by conventional F/STS. To leave margin, micro-aspheric arrays with an AR of 0.11 are fabricated by OTS, and micro-aspheric arrays with an AR of 0.04 are fabricated by slow tool servo (STS), whose coefficient is shown in Table 1. The machining parameters are detailed in Table 2.

The workpiece dimension is 40 × 10 mm^2. As the basic dimension of each lenslet cell is only 0.35 × 0.35 mm^2, the workpiece is large enough to cover hundreds of lenslet cells. In the present study, the dimension of the whole MOAs is 3.5 × 3.5 mm2 covering one hundred lenslet cells.

Micro-freeform optics with more complicated structures, namely radiant micro-structure arrays, are fabricated using the same machining parameters to further validate the superiority of the proposed OTS. The radiant micro-structure arrays can be regarded as a spheric surface imposed by radiant micro-structures, which can be expressed in the local cylindrical coordinate system by:

$$z(\rho,\varphi)=\sqrt{R_{ball}^{\ 2}-\rho^2}-\sqrt{R_{ball}^{\ 2}-R_l^{\ 2}}+A\sin(6\varphi) \tag{11}$$

where R_{ball} is the radius of the spheric surface, R_l denotes the radius of the lenslet, A is the amplitude of the radiant micro-structures. The coefficients of the radiant micro-structure arrays are shown in Table 3.

Table 3. Coeffecients of the Radiant micro-structure arrays.

Coefficient	Radiant micro-structure arrays
Spheric radius R_{ball} (mm)	0.22
Radius of the array R_l (mm)	0.18
Amplitude A (mm)	0.002

5. Results and discussion

To validate the feasibility of the proposed OTS in the machining of MOAs with high AR, micro-aspheric lens arrays are fabricated by OTS system, and the results are compared with that obtained by conventional F/STS. In addition, micro-freeform lens arrays with radiant micro-structures are also fabricated using OTS to further validate the advantage of OTS for the generation of MOAs with complicated structures.

5.1 Micro-aspheric arrays

Figure 8 shows the features of the micro-aspheric lens arrays generated by OTS. An overview of the generated 4 × 4 lens arrays is shown in Fig. 8(a). It is seen that the lenslet cells are uniformly distributed with equal distance between two successive lenslet cells. A cross-sectional profile passing through the center of the lenslet along *X* direction is shown in Fig. 8(b). Homogeneous characteristics of the shape and size of each lenslet cell can be observed from the 3D topography and the 2D profile.

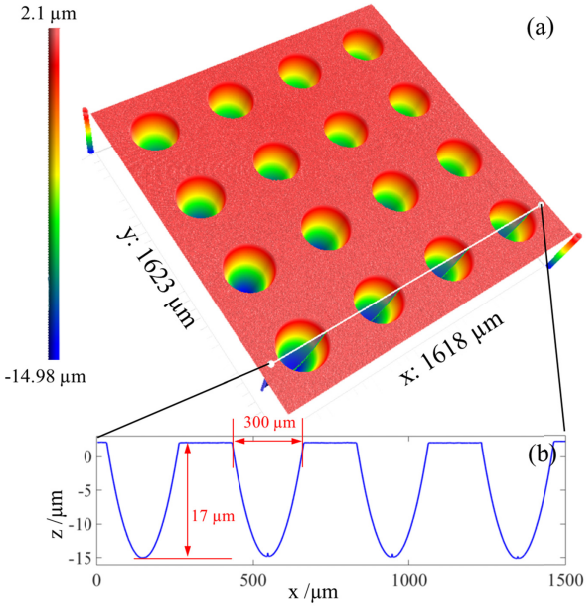

Fig. 8. 3D topographies of (a) the micro-aspheric arrays and (b) the cross-sectional profile in x direction.

As shown in Fig. 8(b), the circumradius and the depth of the lenslet are 150 μm and 17 μm, respectively. According to the definition of AR, the AR of the lenslet is calculated at 0.113, which is equal to the desired AR value as shown in Table 1. As discussed above, using the diamond tool with a clearance angle of 7°, the maximum AR value that can be achieved by conventional F/STS using the diamond tool with a clearance angle of 7° is only 0.06 to avoid tool interference. The micro-aspheric arrays with the AR of 0.113 generated by the proposed OTS cannot be fabricated by the conventional F/STS due to the tool interference, which validates the superiority of the proposed OTS. The capability of OTS in achieving higher AR compared with F/STS is attributed to its unique cutting process, in which each lenslet cell is separately fabricated by a spiral toolpath just like ball milling. This unique machining strategy leads to a totally different the relative position between the diamond tool and the lenslet cell compared with F/STS, as illustrated in Fig. 2. In OTS, the toolpath is smooth without repaid descending movements of the diamond tool, thereby leaving large space between the finished surface and the flank face of the diamond tool.

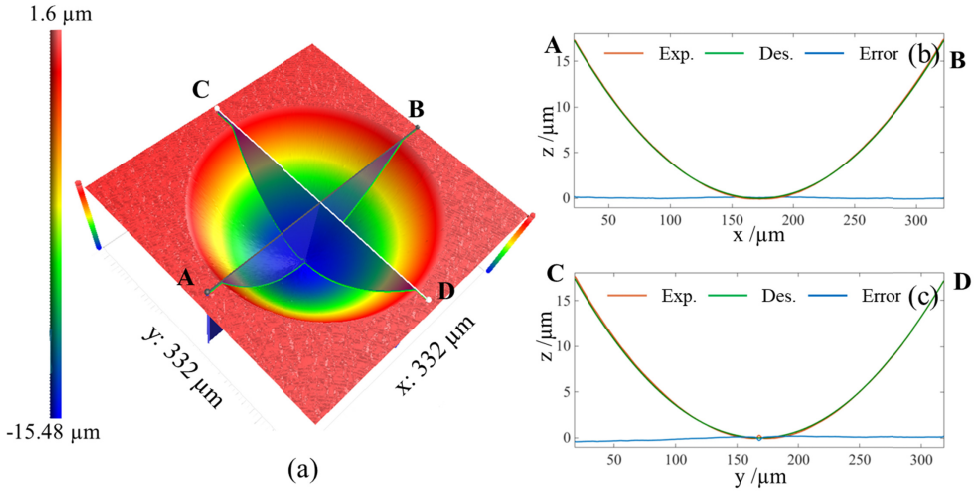

Fig. 9. 3D topographies of (a) generated lenslet cell, (b) and (c) the cross-sectional profiles in *X* and *Y* directions.

To further analysis the shape distortion of the generated MOAs, an arbitrary lenslet cell is selected from the generated lens arrays, whose shape features is shown in Fig. 9. Its cross-sectional profiles along *X* and *Y* directions are extracted and compared with the desired profiles of the lenslet, as shown in Figs. 9(b) and 9(c). As shown in Figs. 9(b) and 9(c), the profile acquired from experiments (in orange color) almost overlaps to the desired profiles (in green color). The shape of the cross-sectional profile of the generated lenslet agrees well with that of the desired lenslet in both *X* and *Y* directions, and the form error is less than ± 50 nm. Overall, it is demonstrated that the feasibility of OTS in the generation of MOAs with high AR and high form accuracy.

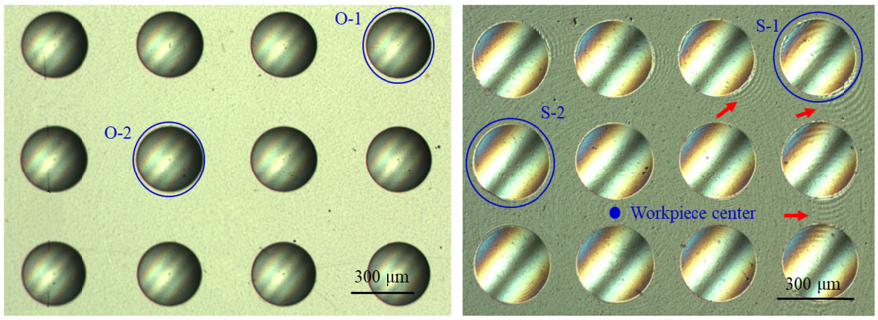

Fig. 10. Microscope images of the MOAs generated by (a) OTS and (b) STS.

Figures 10(a) and (b) show the microscope images of the micro-aspheric lens arrays generated by OTS and STS, respectively. As shown in Fig. 10(a), the whole arrays are characterized as smooth and uniform features without shape and size distortions, which is attributed to the individual cutting process of OTS with the same cutting condition. By removing the spheric surface from the lenslet, the micro-topographies of the lenslet cells named as O-1 and O-2 in Fig. 10(a) are shown in Figs. 11(a) and 11(b), respectively. Even though the two lenslet cells are extracted from different positions of the lens arrays, their surfaces micro-topographies are very similar with the same roughness of 3 nm. Circular residual tool marks with its center overlapping to the center of the lenslet is observed in Figs. 11(a) and 11(b), which results from the unique cutting process of OTS as detailed above.

In contrast, obvious fluctuations along cutting direction were observed on the microscope image of the lens arrays generated by STS, as shown in Fig. 10(b). These undesired fluctuations are majorly caused by the tool tip vibrations in F/STS [16]. In F/STS, each lenslet can be regarded as an impulse excitation of the diamond tool, which can result in the impulse-like acceleration and deceleration of the diamond tool when the tool cuts into and out from each lenslet, as illustrated in Fig. 6(f). The tool vibrations can severely destroy the micro-topography of the generated lenslet and result in a large surface roughness, as illustrated by the micro-topography of the lenslet S-1 in Fig. 11(c). Compared with S-1, much smoother micro-topography is observed for the lenslet S-2 whose position is closer to the center of the workpiece, as shown in Fig. 11(d). The different micro-topographies of S-1 and S-2 is attributed to the radial dependent cutting condition of F/STS. As a result, it is validated that compared with F/STS, the proposed OTS effectively suppress the tool vibrations in the machining of MOAs and enhance the surface uniformity.

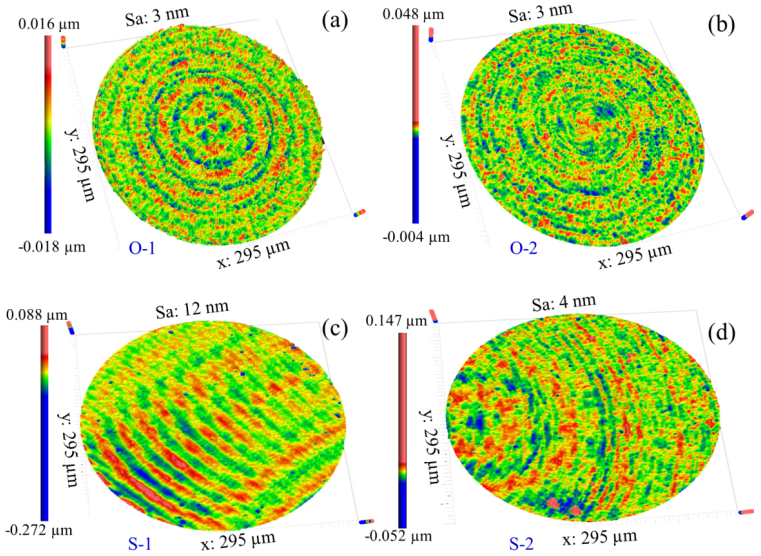

Fig. 11. Micro-topographies of the lenslet cells at different places (a) and (b) generated by OTS and (c) and (d) generated by STS.

According to the principle of OTS system, the *X*- and *Y*-axis harmonically move back and forth in the same frequency of the spindle rotation, in order to generate a local spiral trajectory with its center always coincident with the center of the local lenslet cell. Different from the conventional virtual spindle turning [18], the diamond tool in the OTS system is clamped on the spindle with a fixed offset distance. Accordingly, the amplitudes of the harmonic motions in sine or cosine are equal to the offset distance of the diamond tool, and the amplitudes has no relationship with the aperture of the MOAs. The frequencies of the harmonic motions are equal to the frequency of spindle rotation. Therefore, the spindle speed can remain uniform in the OTS system even in the machining of the optics with large apertures.

The overall cutting time for the MOAs with an area of 3.5 × 3.5 mm^2 is about 4.5 hour. It is known that the constraint for the spindle speed in the servo machining technologies is mostly attributed to the data transfer rate of the control system [27]. To guarantee the form accuracy of each lenslet cell, a large number of control points are required, especially for the lenslet with freeform shapes and with high aspect ratio, which further reduces the spindle speed [28]. This is the common issue for the proposed OTS method and the conventional F/STS. Due to the repeated cutting operation of OTS, the number of the controlling points for OTS is much less than that of conventional F/STS, thereby leading to a relatively higher

machining efficiency. For example, the cutting time for such an area and for such lenslet density in conventional slow tool servo is estimated to be about 8 hours by adopting the same feed rate and proper sampling numbers [17,28]. Higher spindle speed can be selected by using the control system with better data transfer rate.

5.2 Micro-freeform lens arrays

With the fast development of optical and electronical devices, MOAs with simple spheric and aspheric shapes are hard to fulfil the requirements of advanced optical systems for multi-function integration [4,5]. To fulfil the requirements of the functional integration and minimization of the optical system, micro-freeform lens arrays with complicated structures as well as with high aspect ratio are increasingly required, such as micro-Fresnel lens arrays [5] and retroreflective arrays [4]. Due to the tool interference and limited dynamic response, it is difficult for conventional F/STS to fabricated micro-freeform lens arrays with high form accuracy. To validate the flexibility of the proposed OTS system in machining of micro-freeform lens arrays, radiant micro-structure arrays are fabricated. An overview of the generated radiant micro-structure arrays is shown in Fig. 12(a). Each lenslet is characterized as the same features with six radiant lobes. An arbitrary lenslet is extracted from the arrays, whose 3D topography and 2D cross-sectional profile are shown in Figs. 12(b) and 12(c), respectively. The diameter and the depth of lenslet are 365 μm and 17.06 μm, respectively, so the AR of the lenslet is 0.09. The shape of the generated structure agrees well with the desired structure that expressed in Eq. (11) with a slight deviation of 1.3%, which validates the feasibility of the proposed OTS in generation of MOAs with almost arbitrary structures with high form accuracy and no tool interference.

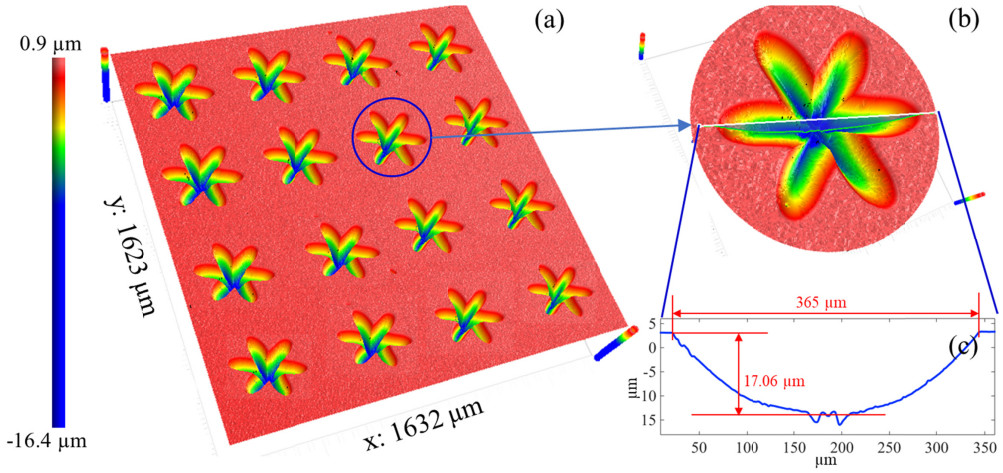

Fig. 12. Topography of the (a) radiant micro-structure arrays generated by OTS and (b) an arbitrary lenslet and (c) cross-sectional profile.

Of note, the radiant micro-structure arrays fabricated by OTS are characterized as discontinuous shapes with high aspect ratio. Although sometimes it is easy for F-/STS to generate the complicatedly shaped surfaces, it is often extremely difficult for the F-/STS using spiral toolpath to generate the correspondingly arrayed structures [18]. In F/STS diamond turning of MOAs, the discontinuous spiral toolpath can induce severe tool vibrations, thereby deteriorating surface roughness and resulting in poor surface quality [16,17]. Especially, the tool vibrations can be more obvious in the machining of MOAs with high AR, owing to the steep descending and rising movements of the diamond tool [18]. Moreover, the non-smooth toolpath with large slope angle in turning of MOAs with high AR inevitably cause the interference between the flank face of the diamond tool and the finished surface.

6. Conclusions

In the present study, a novel offset-tool-servo (OTS) diamond machining technology has been proposed to achieve flexible fabrication of micro-optics arrays (MOAs) with high aspect ratio (AR). Different from conventional fast and slow tool servo (F/STS), the diamond tool is fixed on the spindle with a fixed offset distance from the rotation center. Through the servo motions of three translational axes and a rotational axis, each lenslet is individually fabricated by spiral toolpaths just like ball end milling. This machining approach effectively avoid the tool interference and tool vibration in the fabrication of MOAs with high AR using conventional fast and slow tool servo (F/STS), thereby ensuring the form accuracy and surface uniformity of the generated MOAs. Through considering the offset distance between the diamond tool and the rotation center of the spindle, toolpath determination strategy is proposed. The main conclusions can be summarized as follows:

(1) In OTS, spiral toolpath with its center overlapping to the center of the corresponding lenslet is generated for each lens lenslet. In this case, the toolpath is smooth and continuous without steep descending movement of the tool even in the machining of MOAs with high AR. Attributing to this, MOAs with two times higher AR can be fabricated by OTS compared with conventional F/STS using the same diamond tool.

(2) In OTS, the diamond tool periodically contacts and departs form the workpiece surface, but there is no velocity and acceleration fluctuations of the diamond tool during the machining process. The unique cutting process of OTS well ensures the surface smoothness and uniformity of the generated MOAs.

(3) To validate OTS, micro-aspheric arrays with the AR of 0.113 is fabricated using a diamond tool with a clearance angle of 7°. In comparison, the maximum AR that can be achieved by F/STS is only 0.06 that is much smaller than that of OTS. Compared with F/STS, more uniform and smoother surface quality with roughness of 3 nm is acquired by OTS attributing to its uniform cutting condition.

(4) A kind of freeform lens arrays, namely MOAs with radial structures, are also fabricated by OTS to validate the potential of the proposed OTS in machining of MOAs with complicated shapes as well as with high AR. The good agreement between the generated surface and the desired surface well validates the flexibility of OTS in the machining of MOAs with complicated structures.

Funding

Research Committee of The Hong Kong Polytechnic University (RUNS), Research Grant Council of the Hong Kong Special Administrative Region, China (PolyU152021/17E), and the National Natural Science Foundation of China (NSFC) (51675455).

References

1. H. Zuo, D.-Y. Choi, X. Gai, B. Luther-Davies, and B. Zhang, "CMOS compatible fabrication of micro, nano convex silicon lens arrays by conformal chemical vapor deposition," Opt. Express **25**(4), 3069–3076 (2017).
2. K. Li, A. Ö. Yöntem, Y. Deng, P. Shrestha, D. Chu, J. Zhou, and J. Yao, "Full resolution auto-stereoscopic mobile display based on large scale uniform switchable liquid crystal micro-lens array," Opt. Express **25**(9), 9654–9675 (2017).
3. H. Suzuki, T. Moriwaki, Y. Yamamoto, and Y. Goto, "Precision cutting of aspherical ceramic molds with micro PCD milling tool," CIRP Ann. **56**(1), 131–134 (2007).
4. E. Brinksmeier and L. Schönemann, "Generation of discontinuous microstructures by diamond micro chiseling," CIRP Ann. **63**(1), 49–52 (2014).
5. R. Jasinevicius, J. Duduch, G. Cirino, and P. Pizani, "Diamond turning of small Fresnel lens array in single crystal InSb," J. Micromech. Microeng. **23**(5), 055025 (2013).
6. J. Chen, H. H. Lee, D. Wang, S. Di, and S.-C. Chen, "Hybrid imprinting process to fabricate a multi-layer compound eye for multispectral imaging," Opt. Express **25**(4), 4180–4189 (2017).

7. D. Fattal, Z. Peng, T. Tran, S. Vo, M. Fiorentino, J. Brug, and R. G. Beausoleil, "A multi-directional backlight for a wide-angle, glasses-free three-dimensional display," Nature **495**(7441), 348–351 (2013).
8. C. Wang, C. F. Cheung, M. Liu, and W. B. Lee, "Fluid jet-array parallel machining of optical microstructure array surfaces," Opt. Express **25**(19), 22710–22725 (2017).
9. Z. He, Y.-H. Lee, D. Chanda, and S.-T. Wu, "Adaptive liquid crystal microlens array enabled by two-photon polymerization," Opt. Express **26**(16), 21184–21193 (2018).
10. J. Shao, Y. Ding, W. Wang, X. Mei, H. Zhai, H. Tian, X. Li, and B. Liu, "Generation of fully-covering hierarchical micro-/nano- structures by nanoimprinting and modified laser swelling," Small **10**(13), 2595–2601 (2014).
11. Z. Sun, S. To, and K. M. Yu, "One-step generation of hybrid micro-optics with high-frequency diffractive structures on infrared materials by ultra-precision side milling," Opt. Express **26**(21), 28161–28177 (2018).
12. B. S. Dutterer, J. L. Lineberger, P. J. Smilie, D. S. Hildebrand, T. A. Harriman, M. A. Davies, T. J. Suleski, and D. A. Lucca, "Diamond milling of an Alvarez lens in germanium," Precis. Eng. **38**(2), 398–408 (2014).
13. Z. Li, F. Fang, J. Chen, and X. Zhang, "Machining approach of freeform optics on infrared materials via ultra-precision turning," Opt. Express **25**(3), 2051–2062 (2017).
14. Z. Sun, S. To, and S. Zhang, "A novel ductile machining model of single-crystal silicon for freeform surfaces with large azimuthal height variation by ultra-precision fly cutting," Int. J. Mach. Tools Manuf. **135**, 1–11 (2018).
15. G. E. Davis, J. W. Roblee, and A. R. Hedges, "Comparison of freeform manufacturing techniques in the production of monolithic lens arrays," in *Optical Manufacturing and Testing VIII*, (International Society for Optics and Photonics, 2009), 742605.
16. Z. Zhu, S. To, W.-L. Zhu, and P. Huang, "Feasibility study of the novel quasi-elliptical tool servo for vibration suppression in the turning of micro-lens arrays," Int. J. Mach. Tools Manuf. **122**, 98–105 (2017).
17. Z. Zhu, S. To, and S. Zhang, "Large-scale fabrication of micro-lens array by novel end-fly-cutting-servo diamond machining," Opt. Express **23**(16), 20593–20604 (2015).
18. S. To, Z. Zhu, and H. Wang, "Virtual spindle based tool servo diamond turning of discontinuously structured microoptics arrays," CIRP Ann. **65**(1), 475–478 (2016).
19. P. Huang, S. To, and Z. Zhu, "Diamond turning of micro-lens array on the roller featuring high aspect ratio," Int. J. Adv. Manuf. Technol. **96**(5-8), 2463–2469 (2018).
20. D. W. K. Neo, A. S. Kumar, and M. Rahman, "An automated Guilloche machining technique for the fabrication of polygonal Fresnel lens array," Precis. Eng. **41**, 55–62 (2015).
21. Z. Zhu, S. To, and S. Zhang, "Theoretical and experimental investigation on the novel end-fly-cutting-servo diamond machining of hierarchical micro-nanostructures," Int. J. Mach. Tools Manuf. **94**, 15–25 (2015).
22. X. Zhou, Y. Weng, Y. Peng, G. Chen, J. Lin, Q. Yan, Y. Zhang, and T. Guo, "Design and fabrication of square micro-lens array for integral imaging 3D display," Optik (Stuttg.) **157**, 532–539 (2018).
23. C. C. Chiu and Y. C. Lee, "Fabricating of aspheric micro-lens array by excimer laser micromachining," Opt. Lasers Eng. **49**(9-10), 1232–1237 (2011).
24. L. Li and Y. Y. Allen, "Microfabrication on a curved surface using 3D microlens array projection," J. Micromech. Microeng. **19**(10), 105010 (2009).
25. Z. Zhu, X. Zhou, D. Luo, and Q. Liu, "Development of pseudo-random diamond turning method for fabricating freeform optics with scattering homogenization," Opt. Express **21**(23), 28469–28482 (2013).
26. D. Yu, Y. Wong, and G. Hong, "Ultraprecision machining of micro-structured functional surfaces on brittle materials," J. Micromech. Microeng. **21**(9), 095011 (2011).
27. Z. Zhu and S. To, "Adaptive tool servo diamond turning for enhancing machining efficiency and surface quality of freeform optics," Opt. Express **23**(16), 20234–20248 (2015).
28. W. Gao, T. Araki, S. Kiyono, Y. Okazaki, and M. Yamanaka, "Precision nano-fabrication and evaluation of a large area sinusoidal grid surface for a surface encoder," Precis. Eng. **27**(3), 289–298 (2003).

14.0.171.14 {ts '2020-04-28 05:49:32'}